GEOPHYSICAL RESEARCH LETTERS, VOL. 34, L08805, doi:10.1029/2007GL029253, 2007

On the twilight zone between clouds and aerosols

Ilan Koren,[1] Lorraine A. Remer,[2] Yoram J. Kaufman,[2,3] Yinon Rudich,[1] and J. Vanderlei Martins[2,4]

Received 6 January 2007; revised 15 February 2007; accepted 20 March 2007; published 18 April 2007.

[1] Cloud and aerosols interact and form a complex system leading to high uncertainty in understanding climate change. To simplify this non-linear system it is customary to distinguish between "cloudy" and "cloud-free" areas and measure them separately. However, we find that clouds are surrounded by a "twilight zone" – a belt of forming and evaporating cloud fragments and hydrated aerosols extending tens of kilometers from the clouds into the so-called cloud-free zone. The gradual transition from cloudy to dry atmosphere is proportional to the aerosol loading, suggesting an additional aerosol effect on the composition and radiation fluxes of the atmosphere. Using AERONET data, we find that the measured aerosol optical depth is higher by 13% ± 2% in the visible and 22% ± 2% in the NIR in measurements taken near clouds relative to its value in the measurements taken before or after, and that 30%−60% of the free atmosphere is affected by this phenomenon. **Citation:** Koren, I., L. A. Remer, Y. J. Kaufman, Y. Rudich, and J. V. Martins (2007), On the twilight zone between clouds and aerosols, *Geophys. Res. Lett.*, *34*, L08805, doi:10.1029/2007GL029253.

1. Introduction

[2] *Squires* [1956] showed that anthropogenic pollution from ship tracks can generate thin clouds in an otherwise cloud free and clean atmosphere. Since then, we found that clouds and aerosols (natural or pollution particles suspended in the air) play a critical role in determining cloud cover, precipitation, evaporation, and the response of the climate system to anthropogenic emissions [*Gunn and Phillips*, 1957; *Ramanathan et al.*, 2001; *Kaufman et al.*, 2002].

[3] Clouds are defined as clusters of condensed droplets formed when aerosol particles are activated to droplets in a super saturated environment. However it is not clear what is the minimal amount of condensed water that could be considered a cloud. Discriminating between aerosols and clouds and the demarcation of cloud boundaries have been exceedingly difficult independent of the measurement system employed. We suggest that the shift between clouds to cloud-free atmosphere contains an additional component, a "Twilight Zone" or a gradual transition zone that depends on both the presence of nearby clouds and on the aerosol loading. Here we use the term "twilight" for its less technical definition, which according to *Merriam-Webster's Collegiate Dictionary* (9th edition) is: "an intermediate state that is not clearly defined or a period of decline." This transition zone is currently classified as cloud-free by most observing systems, but since algorithms that invert aerosol properties are sensitive to cloud contamination, most retrieval algorithms will be biased toward data that is far from clouds and therefore, will miss some of the contribution of this zone. Furthermore, the possible effects of this zone are not included in chemical transport models used to estimate the aerosol direct forcing, possibly leading to discrepancies between models and measurements [*Yu et al.*, 2006].

[4] Figure 1a shows a small dissipating cloud. Subtracting the background reflectance, mostly Rayleigh scattering, causes the background to become black (Figure 1b). Then by masking out the obvious cloud pixels and stretching the dynamic range (to be sensitive to low reflectance), it is clearly shown that the cloud's optical influence extends far beyond the borders of the cloud (Figure 1c). Other cloud masks could be defined, but there is no perfect mask that will unambiguously determine the cloud.

[5] Halos of enhanced humidity around clouds were shown by in situ measurements and clouds resolving models [*Radke and Hobbs*, 1991; *Kollias et al.*, 2001]. These high humidity halos have been found to occur more on the down-shear side of cumulus clouds [*Lu et al.*, 2002, 2003] extending to distances of several cloud radii for small cumulus clouds, up to 1 km from the cloud [*Perry and Hobbs*, 1996].

[6] The "twilight zone" discussed here extends for tens of kilometers and is better described as the property of the cloud field. Clouds in the present analysis are used as markers for an area with potential undetected, thin, sparse clouds and humidified aerosols. We assume that the probability for the existence of such clouds and humidified aerosols is higher in the vicinity of detectable clouds.

2. Analysis

[7] As an example, we show the presence of the twilight zone in MODIS imagery. We apply the MODIS aerosol algorithm to identify clouds based on spatial variability [*Martins et al.*, 2002]. Figure 2 shows one example over the Atlantic Ocean. Looking only at the cloud-free regions we find a systematic reduction in the reflectance as a function of the distance from the nearest cloud (Figure 2, right). We calculate reflectance as a function of distance from the nearest cloud for 20 such cases over the global oceans during all seasons for different cloud fields and aerosol loadings. The average reflectance for the 20 MODIS cases 3 km from the clouds compared to the reflectance 20 km away from the nearest cloud (with standard error) are 5.6% ± 0.1%, 10.6% ± 0.1% and 13.0% ± 0.1% higher for

[1]Department of Environmental Sciences Weizmann Institute, Rehovot, Israel.
[2]NASA Goddard Space Flight Center, Greenbelt, Maryland, USA.
[3]Deceased 31 May 2006.
[4]Department of Physics and Joint Center for Earth Systems Technology, University of Maryland Baltimore County, Baltimore, Maryland, USA.

0094-8276/07/2007GL029253$05.00

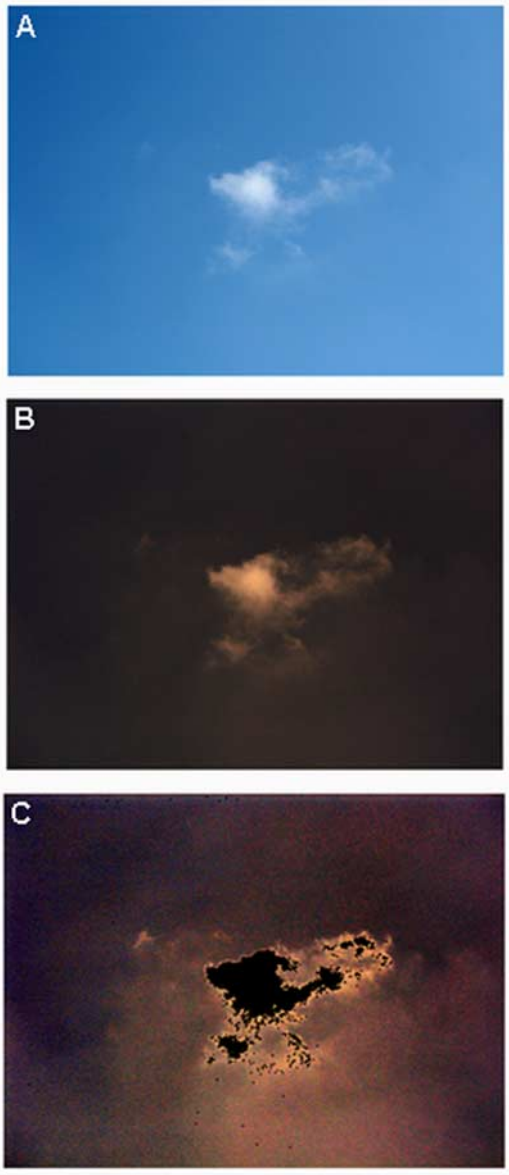

Figure 1. An image of a cloud and the "twilight zone" taken from the ground using a digital camera: (a) true color image of an isolated dissipating cumulus cloud; (b) background gradients caused mostly by molecular scattering were removed; and (c) by masking out the obvious cloud pixels the new dynamic range allows to see the extent of the twilight zone and how the clear sky is not so clear.

0.47 μm, 0.66 μm and 2.13 μm, respectively. The precision and small standard errors are due to the large statistical base (1000's per case) from which the averages are calculated.

[8] Analyzing MODIS data in order to define the twilight climatology requires analysis of many data granules for many different cloud fields and aerosols. Moreover it is hard to rule out alternative processes and instrumental artifacts that may contribute to the enhanced reflectance in the vicinity of clouds. For example, cloud 3D effects, namely photons escaping from the side of the cloud scattered toward the satellite by air molecules and aerosols may result in higher reflectance near clouds [*Wen et al.*, 2006]. Likewise instrumental stray light may contribute to some of the enhancement within the first 3 km of the cloud [*Meister et al.*, 2005; B. Franz and G. Meister, MODIS/Aqua stray light flagging and masking, NASA Goddard Space Flight Center, Greenbelt, Md., available at http://oceancolor.gsfc.nasa.gov/REPROCESSING/Aqua/R1/modisa_repro1_stlight.html, 2005]. Nevertheless these two effects happen in a spatial scale smaller than the twilight zone phenomenon we show in Figure 2.

[9] To avoid these issues we use data from the Aerosol Robotic global network (AERONET) of ground-based Sun photometers [*Holben et al.*, 1998]. Artifacts caused by near cloud scattering are negligible in comparison with the brightness of viewing the solar disk. Also the optical collimator on the AERONET instrument reduces stray light artifacts. The AERONET instruments collect data in intervals no longer than 15 minutes, unless a cloud blocks the direct view of the sun – an indication of cloud presence. Thus we use the absence of a sun measurement at the appointed time as a proxy for the presence of a cloud [*Kaufman and Koren*, 2006]. For selected AERONET stations we accumulated all the data for the entire length of the data record restricting it to high sun (10 am to 2 pm). Several years of data were combined into one data set, but individual stations were processed separately. Every sun observation was tagged as to the time interval between the observation and the nearest cloud, remembering that a cloud is present when a sun observation is expected, but does not occur. The data were then sorted with respect to the time to the nearest cloud, and the ensemble mean AOD and Angstrom exponent were calculated as a function of this interval. Angstrom exponent is defined using two wavelengths (440 nm and 870 nm), and is a measure of particle size (*Eck et al.*, 1999).

[10] Figure 3 shows for one biomass burning station (Alta-Floresta, Brazil, 2000–2006) the linear decay of the aerosol optical depth (AOD) and the increase in Angstrom exponent as a function of the logarithm of the time from the closest detectable cloud. The increase in the Angstrom exponent shows that particles are smaller the further in time from a detectable cloud.

[11] AERONET data were analyzed for 3–5 years of data from 15 stations around the globe with different cloud fields and aerosols. The analyzed stations were grouped into three types of aerosols: (1) stations in the Amazon during the dry season where meteorological conditions are relatively stable. The area is under the influence of a regional high-pressure system above a surface boundary layer and is associated with lower precipitation, land clearing, and biomass burning [*Nobre et al.*, 1998]. (2) Clean stations at isolated islands where the aerosol loading is very small and is mostly sea salt and marine sulfates, and (3) stations from locations with high loadings of industrial and urban pollution.

[12] At all Aeronet stations studied here the averaged AOD decreased linearly with the logarithm of the time from the nearest cloud. For each station we have calculated the slope (the decay rate) of the aerosol optical depth AOD vs. the logarithm of the time T from the last detectable cloud, $\frac{d(AOD)}{d\ln T}$ (Figure 4a) and the Angstrom exponent, Å, as a function of time from the nearest cloud (Figure 4b). The estimated standard error of the averaged AOD as a function of the time of the measurement is on the order of 2.5% for all stations, the errors for Å are about 5% and the error of the slopes for each station are on the order of 4%.

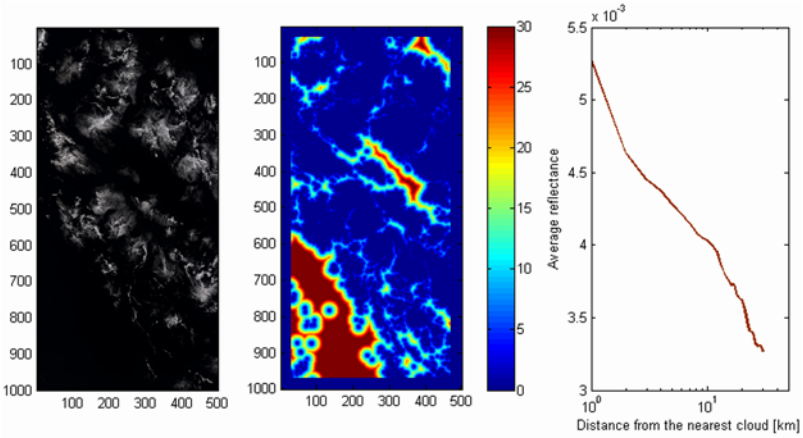

Figure 2. Reflectances as a function of the distance from the nearest cloud: (left) true color image of a cumulus cloud field over the Atlantic Ocean; (middle) distance to the nearest cloud in km (color scale saturated on distance larger than 30 km); and (right) average reflectance of MODIS NIR channel (870 nm) of the cloud free atmosphere as a function of the distance to the nearest cloud in km.

[13] The results, summarized in Figure 4, clearly indicate that:

[14] (1) There is a systematic increase in the aerosol optical depth AOD as the time interval between the measurements and the nearest cloud decreases, represented by negative slopes for all 15 stations.

[15] (2) Systematically lower values of the Angstrom exponent are observed closer to the clouds (Figure 4b), suggesting greater contribution of large particles or undetected cloud to the observed AOD nearer the cloud.

[16] (3) A stronger increase in AOD when approaching the cloud is observed in more polluted environment. The slope $\frac{d(AOD)}{d\ln T}$ is systematically larger (Figure 4a) when the aerosol loading of the environment is higher.

3. Discussion

[17] What is causing the enhancement of radiance and AOD near clouds? Clouds or humidified aerosols? The answer to this question is clearly 'both'. The uncertainty

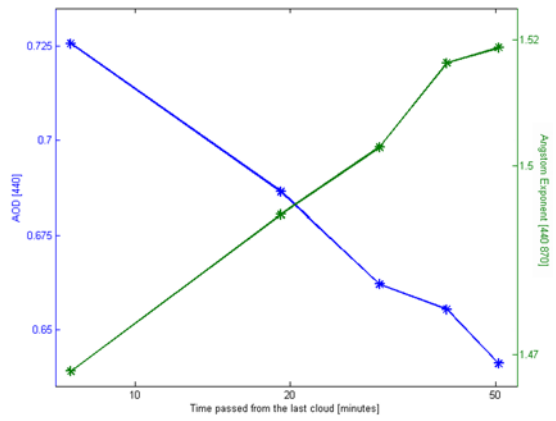

Figure 3. An analysis of AERONET data for Alta-Floresta (Brazil) during the biomass (dry) season 2000–2004, as a function of the estimated distance from the nearest cloud. Blue, AOD at 440 nm; green, Angstrom exponent (440, 870). Standard error of the averaged AOD's is 2% and of the Angstrom exponent 3% for this station.

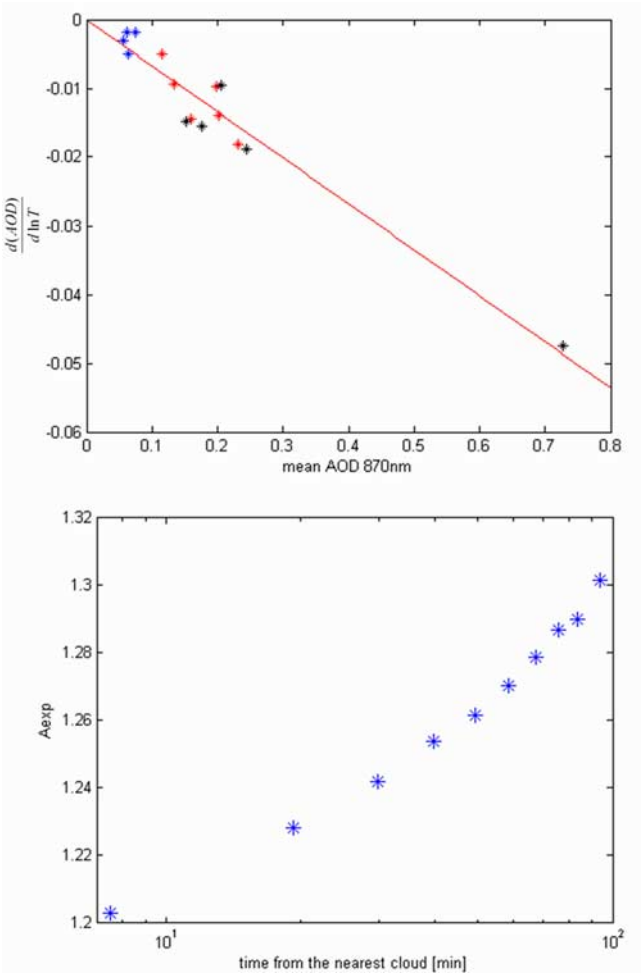

Figure 4. (a) Changes of the slope $\frac{d(AOD)}{d\ln T}$ as a function of the aerosol loading at the station. More aerosols, as represented by the optical depth, are associated with steeper slopes. (b) Averaged Angstrom exponent for the 15 stations as a function of time from the nearest cloud. Transition toward larger exponents far from the clouds indicates a transition to finer (drier) aerosols with lesser contribution from clouds.

of distinguishing between 'cloud' and 'cloud-free' is an inherent property of the nature of the atmosphere and does not depend on the method by which one detects clouds. Any cloud detection method that attempts to classify observations as either cloud or cloud-free will encounter a "gray area" where the cloud signal is weak. This includes spectral and spatial tests for remote sensing and droplet concentration thresholds for in situ measurements.

[18] In this paper we use detectable clouds as a tracer for undetectable clouds. The basic assumption is that in the vicinity of a cloud field some of the clouds are detectable and some are undetectable due to their weak signature. Therefore, the probability for existence of an undetectable cloud is correlated with the distance or time from the nearest detectable cloud.

[19] It is also expected that the relative humidity will be enhanced near clouds, creating an environment where aerosols uptake water and eventually deliquesce, becoming larger and more optically efficient. Therefore, we expect to find both undetectable clouds and humidified aerosols closer to detectable clouds, and as the distance and time from the nearest cloud field increases, the free atmosphere will contain fewer clouds and drier (and hence smaller) aerosols.

[20] Characteristics of the cloud and its environment will determine the extent of the cloud's influence. A forming cumulus cloud with strong updrafts in the center and downdrafts in the periphery may not create an extensive "twilight zone" in its vicinity due to drying air produced by the downdrafts. The same cloud 10 to 20 minutes later will start to disperse producing the mix of enhanced humidity and evaporating cloud droplets. Therefore, to measure the cloud twilight zone, sufficient statistics of cloud fields must be obtained.

[21] Satellite images are snapshots of cloud fields that sample clouds in all stages of development, including those that result in the signal we call "twilight". Likewise, AERONET observations may encounter a cloud during any stage of its development, including high humidity situations and cloud dissipation. The transition from detectable clouds to dry aerosol can be observed both in the spatial and temporal domain.

[22] How significant and what is the extent of this continuum and enhanced AOD from a global perspective? The 15 AERONET stations analyzed here show a mean decrease in the AOD from the first sample measured near a cloud to the second sample (less than 15 minutes later) to be $13\% \pm 2\%$ in the blue (440 nm) and $22\% \pm 2\%$ in the near IR (870 nm), where the stated uncertainty is the standard error. The drop in AOD from the nearest cloud measurement to the third sample (less than 30minutes later) is $15\% \pm 2\%$ and $27\% \pm 2\%$ for the 440 nm and the 870 nm, respectively. The first two samples occupy more than 60% of the clear sky and the first three close to 70% of the clear sky in the data base (i.e. 70% of the data is within 45 minutes of a cloud).

[23] For the spatial domain we use the MODIS analysis. Although we advise caution in using satellite data to estimate twilight zone effects, the similar dependence of the AOD in the time domain in AERONET data suggests that most of the signal shown in the MODIS images is real and is not instrumental nor a 3D effect. This is especially true 3 km and more from clouds (far from stray light issues), and when using the 2.1 μm channel, which is less susceptible to 3D effects. From the 20 MODIS datasets analyzed we see that the enhanced reflectance decays up to 30 km away from the nearest cloud (Figure 2) with an e-folding distance of 10 km.

[24] The significance of the area of such a belt around clouds will depend heavily on the global spatial distribution of clouds. Theoretically, if the global cloud fraction is assumed to be 50% and is concentrated in one cloud, then a border of 10 km around this cloud would occupy only 0.1% of the globe (570000 km^2). But for realistic cloud distributions the enhancement zone is much larger. In order to estimate the true area, we use global cloud satellite data of a few days and estimate the average area of a border with width of 10 km around the detectable clouds. For average global cloud fraction of 0.51 the area of the 10 km border covers 17% of the globe (34% of the cloud-free area) and a border of 30 km width covers 30% of the globe (60% of the cloud-free area).

[25] We show the signature of undetectable clouds and humidified aerosols – the twilight zone - in two data sets. We average a large number of MODIS reflectance measurements together as a function of distance from the nearest cloud and show enhanced reflectance in the vicinity of clouds. This enhanced reflectance decays linearly with the logarithm of the distance from the nearest cloud and extends tens of kilometers into the "cloud-free" atmosphere. The same phenomenon, translated as enhanced AOD, is also shown in the AERONET data, at different stations in very different aerosol and cloud regimes. The enhanced reflectance is characterized by elevated AOD and larger particles, and represents a continuum regime linking detectable clouds through undetectable clouds and humidified aerosol to a dry fine particle aerosol far from the cloud field. The strength of the effect depends on the aerosol loading. We estimate that this continuum is significant in 30 to 60% of the globe that is now labeled "cloud-free", and has important consequences for estimates of aerosol forcing. We have estimated that due to the fractal cloud distribution, the area within a few kilometers of the nearest cloud occupies a large portion of the free atmosphere, and we speculate that AOD is most likely underestimated in satellite retrievals due to biases towards measurements in cloud-free environments. Therefore the total aerosol direct forcing may be significantly higher than is currently estimated due to large contributions from this transition zone.

[26] **Acknowledgments.** This paper is dedicated to the memory of Yoram J. Kaufman, a dear friend and a brilliant scientist. We are thankful to Tom Eck and Graham Feingold for their great comments and to the numerous AERONET site principal investigators for their efforts in establishing and maintaining the sites. This research was supported in part by the Israel Science Foundation (grant 1355/06). I.K. is incumbent of the Benjamin H. Swig and Jack D. Weiler career development chair.

References

Eck, T. F., B. N. Holben, J. S. Reid, O. Dubovik, A. Smirnov, N. T. O'Neill, I. Slutsker, and S. Kinne (1999), Wavelength dependence of the optical depth of biomass burning, urban, and desert dust aerosols, *J. Geophys. Res.*, *104*, 31,333–31,349.

Gunn, R., and B. B. Phillips (1957), An experimental investigation of the effect of air pollution on the initiation of rain, *J. Meteorol.*, *14*, 272–280.

Holben, B. N., et al. (1998), AERONET—A federated instrument network and data archive for aerosol characterization, *Remote Sens. Environ.*, *66*, 1–16.

Kaufman, Y. J., and I. Koren (2006), Smoke and pollution aerosol effect on cloud cover, *Science*, *313*, 655–658.

Kaufman, Y. J., D. Tanre, and O. Boucher (2002), A satellite view of aerosols in the climate system—Review, *Nature*, *419*, 215–223.

Kollias, P., B. A. Albrecht, and F. D. Marks (2001), Raindrop sorting induced by vertical drafts in convective clouds, *Geophys. Res. Lett.*, *28*, 2787–2790.

Lu, M.-L., R. A. McClatchey, and J. H. Seinfeld (2002), Cloud halos: Numerical simulation of dynamical structure and radiative impact, *J. Appl. Meteorol.*, *41*, 832–848.

Lu, M.-L., J. Wang, A. Freedman, H. H. Jonsson, R. C. Flagan, R. A. McClatchey, and J. H. Seinfeld (2003), Analysis of humidity halos around trade wind cumulus clouds, *J. Atmos. Sci.*, *60*, 1041–1059.

Martins, J. V., D. Tanré, L. Remer, Y. Kaufman, S. Mattoo, and R. Levy (2002), MODIS cloud screening for remote sensing of aerosols over oceans using spatial variability, *Geophys. Res. Lett.*, *29*(12), 8009, doi:10.1029/2001GL013252.

Meister, G., B. A. Franz, K. Turpie, and C. R. McClain (2005), The MODIS aqua point-spread function for ocean color bands, paper presented at 9th International Symposium on Physical Measurements and Signatures in Remote Sensing, Inst. of Geogr. Sci. and Nat. Resour. Res., Chin. Acad. of Sci., Beijing.

Nobre, A. C., L. F. Mattos, C. P. Dereczynski, T. A. Tarasova, and V. Trosnikov (1998), Overview of atmospheric conditions during the Smoke, Clouds, and Radiation-Brazil (SCAR-B) field experiment, *J. Geophys. Res.*, *103*, 31,809–31,820.

Perry, K. D., and P. V. Hobbs (1996), Influences of isolated cumulus clouds on the humidity of their surroundings, *J. Atmos. Sci.*, *53*, 159–174.

Radke, L. F., and P. V. Hobbs (1991), Humidity and particle fields around some small cumulus clouds, *J. Atmos. Sci.*, *48*, 1190–1193.

Ramanathan, V., P. J. Crutzen, J. T. Kiehl, and D. Rosenfeld (2001), Aerosols, climate and the hydrological cycle, *Science*, *294*, 2119–2124.

Squires, P. (1956), The micro-structure of cumuli in maritime and continental air, *Tellus*, *8*, 443–444.

Wen, G., A. Marshak, and R. F. Cahalan (2006), Impact of 3D clouds on clear sky reflectance and aerosol retrieval in a biomass burning region of Brazil, *IEEE Geosci. Remote Sens. Lett.*, *3*, 169–172.

Yu, H., et al. (2006), A review of measurement-based assessments of aerosol direct radiative effect and forcing, *Atmos. Chem. Phys.*, *6*, 613–666.

I. Koren and Yinon Rudich, Department of Environmental Sciences Weizmann Institute, Rehovot 76100, Israel. (ilan.koren@weizmann.ac.il)

J. V. Martins and L. A. Remer, NASA Goddard Space Flight Center, Code 613.2, Greenbelt, MD 20771, USA.